Expanded View Figures

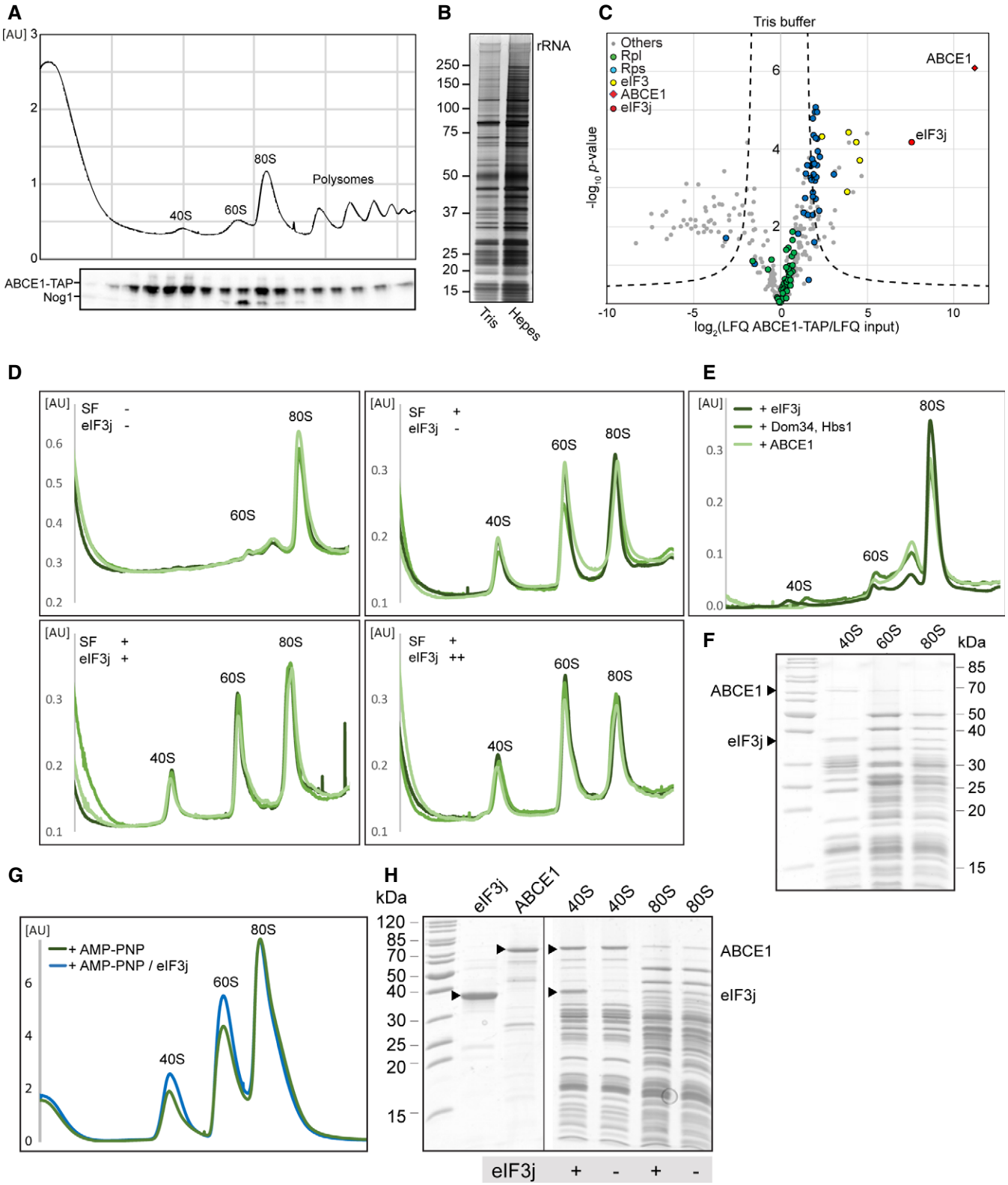

Figure EV1.

Figure EV1. Enrichment of ABCE1 and eIF3j on 40S complexes and assessment of their role in splitting of 80S ribosomes.

A Total cellular extracts from yeast cells expressing ABCE1-TAP were separated on a sucrose gradient (10–50%) by ultracentrifugation. Proteins of each fraction were analyzed by Western blot using a PAP antibody for the detection of the ABCE1-TAP fusion protein and anti-Nog1 antibody to mark the 60S fraction. AU–absorption units at 260 nm.

B Silver-stained NuPAGE gel showing elution from affinity purification using ABCE1-TAP performed in Tris or HEPES buffer (see Materials and Methods for details).

C Volcano plot showing the fold enrichment of proteins in the elution fraction from the ABCE1-TAP purification in Tris buffer followed by mass spectrometry analysis (LC-MS/MS). The enrichment was calculated relative to an "input" corresponding to an aliquot of the ABCE1-TAP cell lysate used for the affinity purification. It is represented, on the x-axis, as $\log_2$(LFQ ABCE1-TAP/LFQ input) where LFQ stands for label-free quantification. The y-axis represents the P-value distribution ($-\log_{10}$-*p*-value) calculated using Student's t-test for all identified proteins represented by a circle. Proteins above the curved lines show a statistically significant enrichment according to the t-test value. The assay was performed in triplicates.

D UV profiles from *in vitro* splitting reaction triplicates with and without splitting factors (SF; ABCE1, Dom34, Hbs1, and eIF6) and eIF3j. Samples were separated on a sucrose gradient (10–50%) by ultracentrifugation. (+) = 4-fold molar excess of eIF3j; (++) = 20-fold molar excess of eIF3j.

E Relative abundance of 80S and subunits in each experiment, as calculated from triplicates shown in (D).

F SDS–PAGE of the 40S, 60S, and 80S peaks obtained from the i*n vitro* splitting experiment (D) containing SFs and high amounts of eIF3j.

G UV profiles from *in vitro* "facilitated" splitting reactions. Samples were separated on a sucrose gradient (10–50%) by ultracentrifugation.

H SDS–PAGE of the input factors (eIF3j and ABCE1) as well as 40S and 80S peaks from the "facilitated" splitting experiment. ABCE1 and eIF3j are marked by arrows, respectively.

Figure EV2. Resolution and model fitting of the human 43S PIC.

A Gold standard Fourier Shell Correlation (FSC) curve for individual bodies in multi-body refinements (40S head including eIF3d, 40S body including eIF3c-NTD and eIF1A, two bodies of the eIF3 PCI-MPN core) and focused refinements using soft binary masks (ABCE1 and the TC).

B Composite map of 40S head and body after multi-body refinement colored and low-pass filtered according to local resolution.

C Composite map of the eIF3 MPN-PCI core (left) after multi-body refinement with two bodies (right), filtered according to local resolution. Structural hallmarks are color coded in the composite map as shown in Fig 5A, and the two bodies are colored according to local resolution.

D Focused refined map of the masked region containing ABCE1, filtered according to local resolution, and colored for ABCE1 (left). Two views are shown colored according to local resolution (right).

E Same as in (D) for eIF1, eIF1A, and the TC.

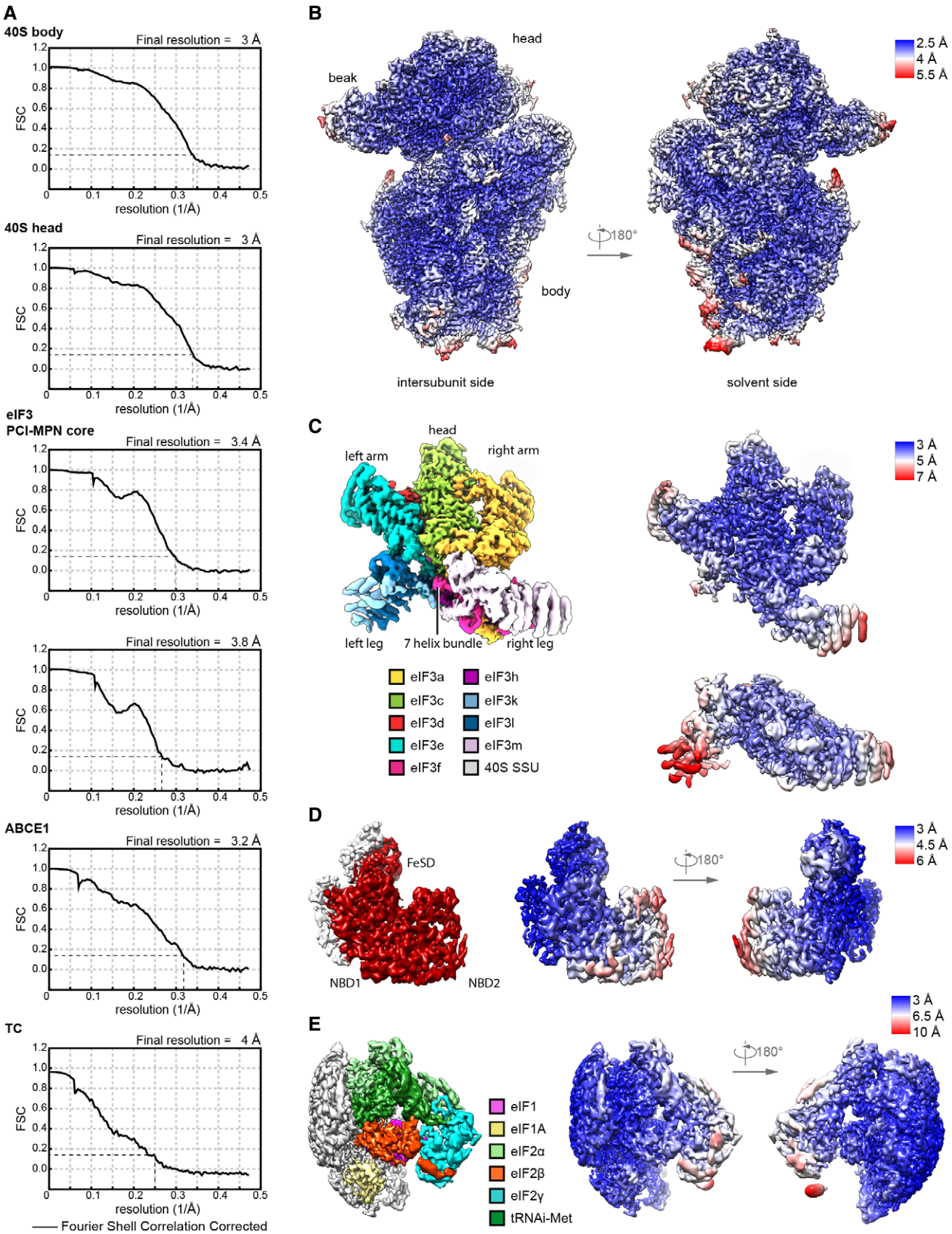
A
40S body
Final resolution = 3 Å
40S head
Final resolution = 3 Å
eIF3
PCI-MPN core
Final resolution = 3.4 Å
Final resolution = 3.8 Å
ABCE1
Final resolution = 3.2 Å
TC
Final resolution = 4 Å
FSC
resolution (1/Å)
Fourier Shell Correlation Corrected
B
head
beak
body
180°
intersubunit side
solvent side
2.5 Å
4 Å
5.5 Å
C
head
left arm
right arm
left leg
7 helix bundle
right leg
eIF3a
eIF3c
eIF3d
eIF3e
eIF3f
eIF3h
eIF3k
eIF3l
eIF3m
40S SSU
3 Å
5 Å
7 Å
D
FeSD
NBD1
NBD2
180°
3 Å
4.5 Å
6 Å
E
eIF1
eIF1A
eIF2α
eIF2β
eIF2γ
tRNAi-Met
180°
3 Å
6.5 Å
10 Å

Figure EV2.

Figure EV3. Density fits of ABCE1 and alignment, model and ribosome binding of human and yeast eIF3j.

A Model for ABCE1 fit into low-pass-filtered density to demonstrate the hybrid semi-open/closed conformation of ABCE1 in native yeast and human 43S PICs.
B Schemes of *H.s.* and *S.c.* eIF3j indicating the length of N- and C-termini; the three helices present in the crystal structure of human eIF3j (PDB 3BPJ) are indicated.
C View highlighting the rearrangement (100-degree rotation) of eIF3 in the human (eIF1A-lacking) and yeast (eIF1A-containing) 43S PICs.
D Alignment between *H.s.* and *S.c.* eIF3j shows 24.6% identity and 53.1% similarity for the full-length protein. Dark blue boxes indicate conservation, light blue boxes indicate similarity. For the sequence (three α-helices) present in the human X-ray structure (PDB 3BPJ from residues 144-213 in protomer 1 and 144-216 in protomer 2), identity/similarity is 32.4%/66.2%, corroborating the reliability of the yeast homology model.
E, F Fits of the human eIF3j crystal structure and the yeast homology model into the corresponding density.
G Interactions of the eIF3j C-terminus (protomer 2) with the 40S head and body shown with models fit into the cryo-EM map of the crosslinked yeast 43S-PIC.
H Schematic representation summarizing interactions of the eIF3j C-terminus with the 40S. Colored boxes indicate residues interacting with eIF3j, with brown representing 18S rRNA, purple representing uS3, and green representing eS10.

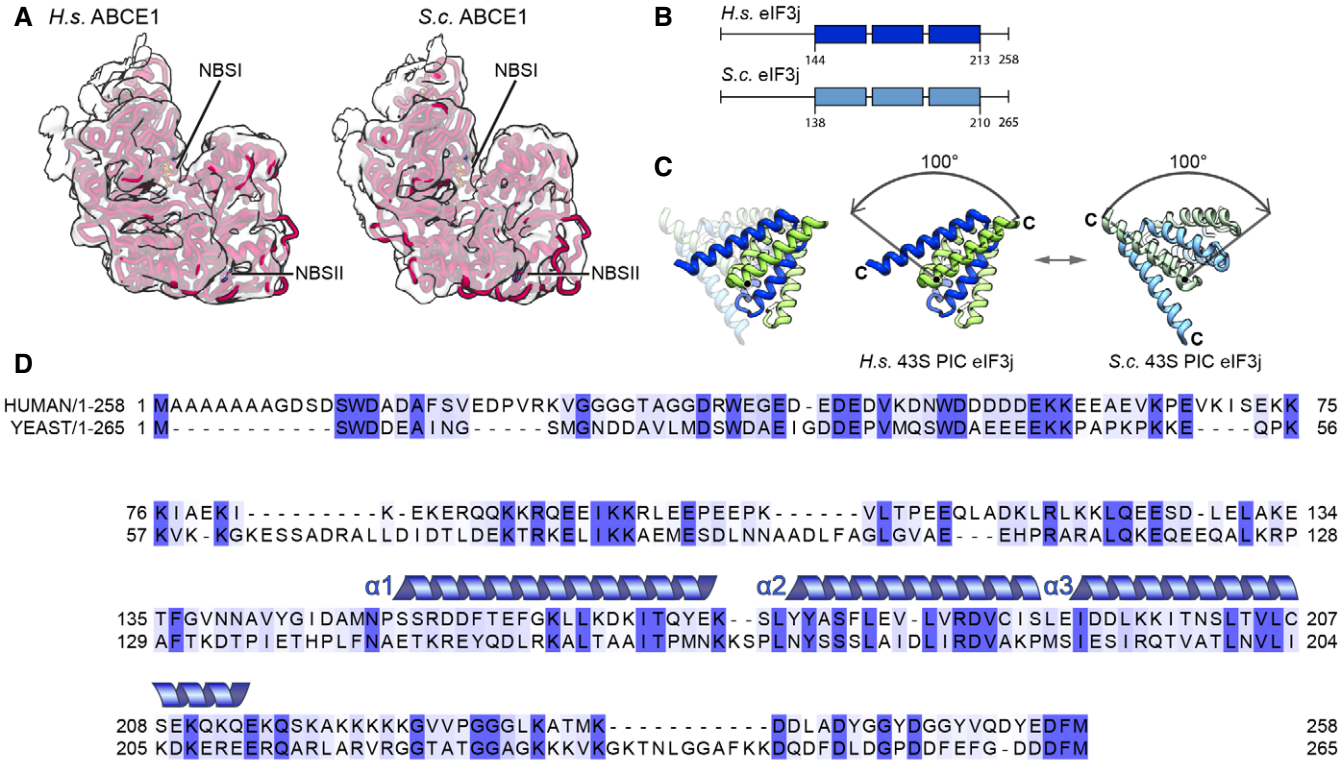
A
H.s. ABCE1
S.c. ABCE1
NBSI
NBSII
B
H.s. eIF3j
144
213 258
S.c. eIF3j
138
210 265
C
100°
H.s. 43S PIC eIF3j
S.c. 43S PIC eIF3j
D
HUMAN/1-258 1 MAAAAAAAGDSDSWDADAFSVEDPVRKVGGGGTAGGDRWEGED-EDEDVKDNWDDDDDEKKEEAEVKPEVKISEKK 75
YEAST/1-265 1 M----------SWDDEAING-----SMGNDDAVLMDSWDAEIGDDEPVMQSWDAEEEEKKPAPKPKKE----QPK 56
76 KIAEKI---------K-EKERQQKKRQEEIKKRLEEPEEPK------VLTPEEQLADKLRLKKLQEESD-LELAKE 134
57 KVK-KGKESSADRALLDIDTLDEKTRKELIKKAEMESDLNNAADLFAGLGVAE---EHPRARALQKEQEEQALKRP 128
α1
α2
α3
135 TFGVNNAVYGIDAMNPSSRDDFTEFGKLLKDKITQYEK--SLYYASFLEV-LVRDVCISLEIDDLKKITNSLTVLC 207
129 AFTKDTPIETHPLFNAETKREYQDLRKALTAAITPMNKKSPLNYSSSLAIDLIRDVAKPMSIESIRQTVATLNVLI 204
208 SEKQKQEKQSKAKKKKKGVVPGGGLKATMK----------DDLADYGGYDGGYVQDYEDFM 258
205 KDKEREERQARLARVRGGTATGGAGKKKVKGKTNLGGAFKKDQDFDLDGPDDFEFG-DDDFM 265
E
H.s. 43S PIC (state II)
eIF3j
FeSD
ABCE1
NBSI
ED
F
S.c. 43S PIC
eIF1A
FeSD
eIF3j
ABCE1
eIF1
G
S.c. 43S PIC XL
uS3
eS10
eIF3j
F59
Y64
h34
G1435
K230
E70
R220
E71
C1220
R218
K236
h18
F243
K244
K245
K231
K234
H
S.c. eIF3j
A1221
K52
E70
E71
G1268
G1435
F59
N
220
225
G576
U581
R V R G G T A T G G A G K 230
h18
K F A G G L N T K G K V K K
245 K
240
235
h34
C
C559
U581
U582
R143
L142
M150
A579
I114
L142
R143
G112
A579
M177
A579
R178
G1438
C1439
U1437
U1266
G1267

Figure EV3.

Figure EV4. Molecular interactions of eIF3d and the PCI-MPN core in the 43S PIC shown with density.

A PCI arc of the PCI-MPN core; zoomed views highlighting fits of the eIF3 PCI arc into the refined density and interactions between the subunits in the PCI-MPN core.

B eIF3a and eIF3c interactions with the 40S.

C Left, Middle: Interactions of the eIF3d N-terminal tail with the PCI-MPN core: Interactions of the ultimate eIF3d N-terminus (Phe4-Pro18) with eIF3e are established *via* Phe4 (to Tyr32 in loop between PCI helices α2 and α3), Gln10 (to His12 in α1), Ile9 and Asp11 (to Arg16 in α2), Ser14 (to Asn164 α9 and Phe132 in α7), Trp16 (to Gly171 in α10), and Gly17 (to Trp170 in α10). eIF3d residues 25-36 are bridging eIF3e and eIF3c. Residues involved are Tyr30 (to Leu208 in eIF3e PCI helix α12), Phe33 (to the peptide backbone of Leu590 in eIF3c α11), and Lys35 (to Gln283 in eIF3e α16). eIF3c-specific interactions are established by Leu39 (to Gln595), Trp45 (Pro603, Ile607, and Glu666), and Thr46 (to Arg641) (see Table S3). For clarity, only density for eIF3d is shown (gray transparent surface). Right: Detailed view of the interaction of F80 (eIF3d) with K36 and R80 (eS27). Density is shown for both proteins (gray transparent surface). Below: MSA of the conserved N-terminal region of eIF3d is shown. Coloring according to default Clustal X color scheme (blue: hydrophobic, magenta: negative charge, red: positive charge, green: polar, orange: glycine, yellow: proline, pink: cysteine, cyan: aromatic).

D Interactions of the eIF3d C-terminal domain with the 40S head and zoomed views of uS7 and eS28 interaction sites shown with density.

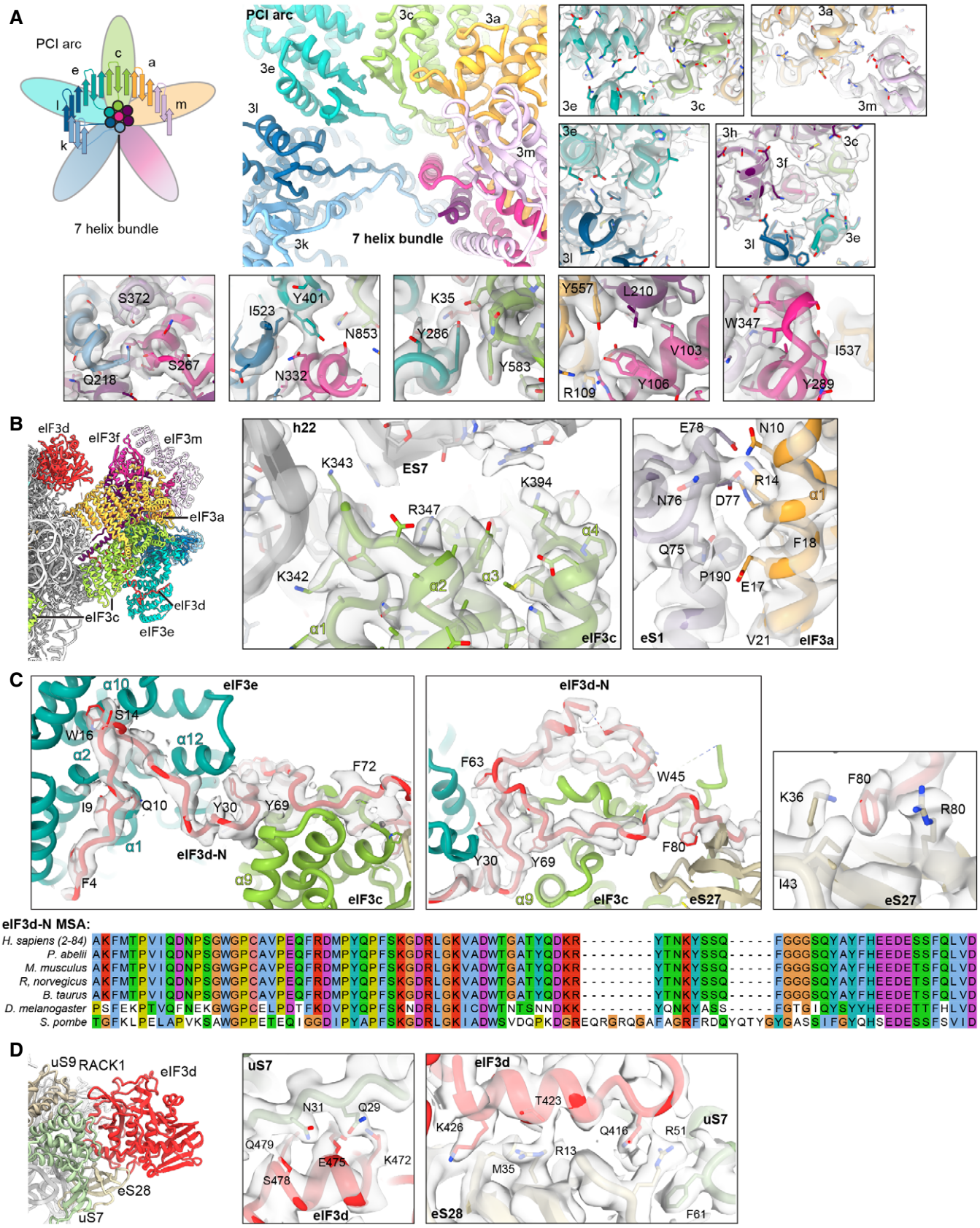
A
PCI arc
c
a
e
l
m
k
7 helix bundle
PCI arc
3c
3a
3e
3l
3m
3k
7 helix bundle
3e
3c
3a
3m
3e
3l
3h
3c
3f
3l
3e
S372
Q218
S267
I523
Y401
N853
N332
K35
Y286
Y583
Y557
L210
V103
R109
Y106
W347
I537
Y289
B
eIF3d
eIF3f
eIF3m
eIF3a
eIF3d
eIF3c
eIF3e
h22
K343
ES7
K394
R347
α4
K342
α2
α3
α1
eIF3c
E78
N10
R14
N76
D77
α1
Q75
F18
P190
E17
eS1
V21
eIF3a
C
α10
eIF3e
S14
W16
α12
α2
F72
I9
Q10
Y30
Y69
α1
eIF3d-N
F4
α9
eIF3c
eIF3d-N
F63
W45
Y30
Y69
F80
α9
eIF3c
eS27
F80
K36
R80
I43
eS27
eIF3d-N MSA:
H. sapiens (2-84) AKFMTPVIQDNPSGWGPCAVPEQFRDMPYQPFSKGDRLGKVADWTGATYQDKR--------YTNKYSSQ-----FGGGSQYAYFHEEDESSFQLVD
P. abelii AKFMTPVIQDNPSGWGPCAVPEQFRDMPYQPFSKGDRLGKVADWTGATYQDKR--------YTNKYSSQ-----FGGGSQYAYFHEEDESSFQLVD
M. musculus AKFMTPVIQDNPSGWGPCAVPEQFRDMPYQPFSKGDRLGKVADWTGATYQDKR--------YTNKYSSQ-----FGGGSQYAYFHEEDETSFQLVD
R, norvegicus AKFMTPVIQDNPSGWGPCAVPEQFRDMPYQPFSKGDRLGKVADWTGATYQDKR--------YTNKYSSQ-----FGGGSQYAYFHEEDETSFQLVD
B. taurus AKFMTPVIQDNPSGWGPCAVPEQFRDMPYQPFSKGDRLGKVADWTGATYQDKR--------YTNKYSSQ-----FGGGSQYAYFHEEDETSFQLVD
D. melanogaster PSFEKPTVQFNEKGWGPCELPDTFKDVPYQPFSKNDRLGKICDWTNTSNNDKK--------YQNKYASS-----FGTGIQYSYYHEEDETTFHLVD
S. pombe TGFKLPELAPVKSAWGPPETEQIGGDIPYAPFSKGDRLGKIADWSVDQPKDGREQRGRQGAFAGRFRDQYQTYGYGASSIFGYQHSEDESSFSVID
D
uS9
RACK1
eIF3d
eS28
uS7
uS7
N31
Q29
Q479
E475
K472
S478
eIF3d
eIF3d
T423
K426
Q416
R51
uS7
R13
M35
eS28
F61

Figure EV4.

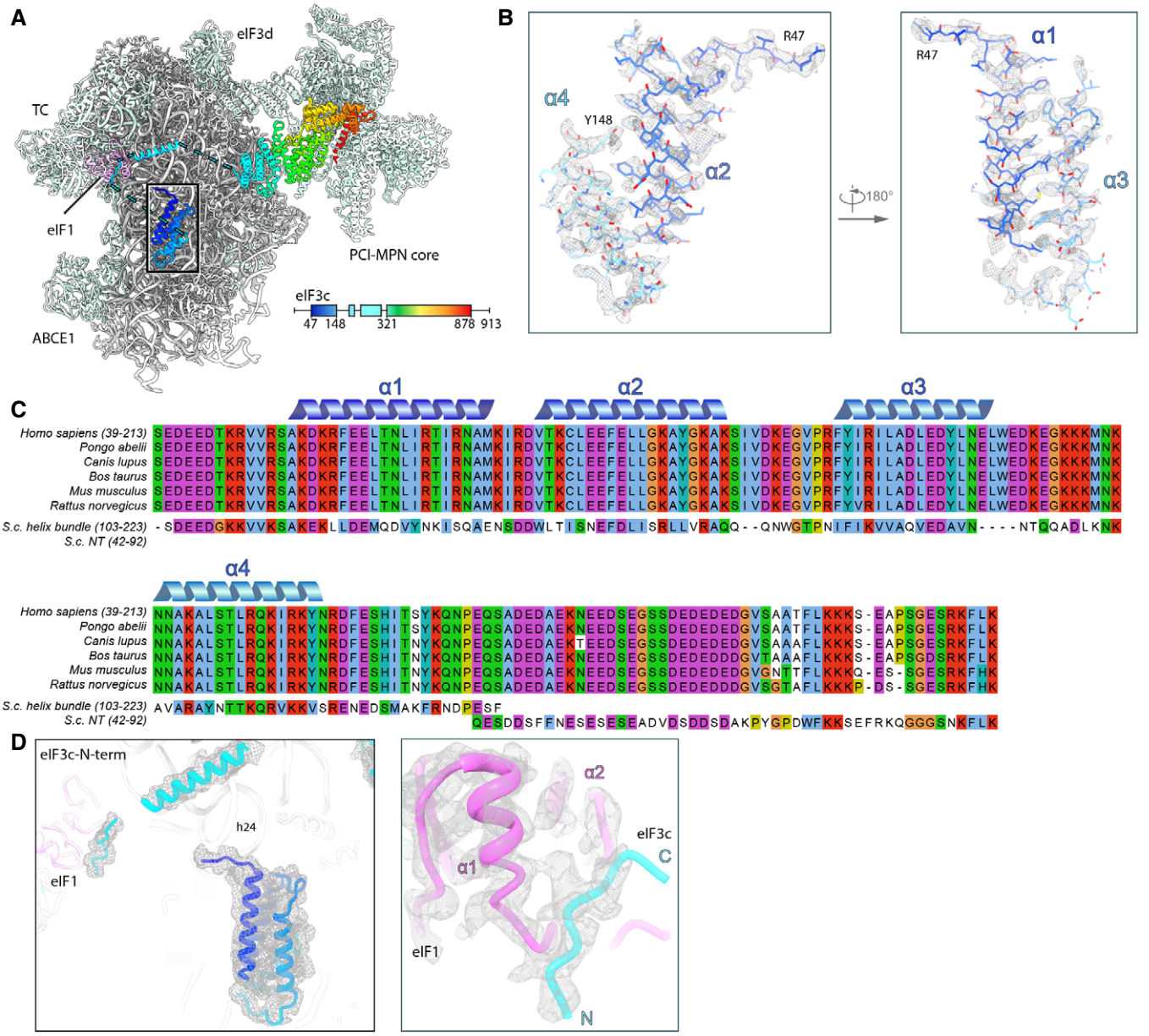

Figure EV5. Model fitting and sequence alignment of the eIF3c-NTD.

A Overview of the TC-containing human 43S PIC as shown in Fig 6 and scheme indicating the parts of eIF3c modeled. Black box indicates section of eIF3c highlighted in (B).

B Zoomed views highlighting fits of the eIF3c-NTD 4-helix bundle into the refined density (gray transparent mesh). The N- and C-terminal residues are marked.

C MSA of the conserved N-terminal region of eIF3c in mammals (Ser39-Lys213 in *H.s.*), aligned with segments of the NTD from *S.c.*. Coloring according to default Clustal X color scheme (blue: hydrophobic, magenta: negative charge, red: positive charge, green: polar, orange: glycine, yellow: proline, pink: cysteine, cyan: aromatic). The 4-helix bundle shows 31.1/67.2% sequence identity/similarity, and the eIF1-interacting stretch present in the N-terminus of *S.c.* eIF3c (Gln42-Lys92) shows 32.0/56.0% sequence identity/similarity with a mammalia-specific insert C-terminal of the conserved 4-helix bundle.

D eIF3c-NTD in the human 43S PIC fitted into the cryo-EM map and zoomed view showing the fit of the eIF1-interacting stretch of eIF3c into the cryo-EM map.